

Nonuniform responses of transmembrane potential during electric field stimulation of single cardiac cells

DAVID KER-LIANG CHENG, LESLIE TUNG, AND ERIC A. SOBIE

Department of Biomedical Engineering, The Johns Hopkins University, Baltimore, Maryland 21205

Cheng, David Ker-Liang, Leslie Tung, and Eric A. Sobie. Nonuniform responses of transmembrane potential during electric field stimulation of single cardiac cells. *Am. J. Physiol.* 277 (*Heart Circ. Physiol.* 46): H351–H362, 1999.— The response of cellular transmembrane potentials (V_m) to applied electric fields is a critical factor during electrical pacing, cardioversion, and defibrillation, yet the coupling relationship of the cellular response to field intensity and polarity is not well documented. Isolated guinea pig ventricular myocytes were stained with a voltage-sensitive fluorescent dye, di-8-ANEPPS (10 μ M). A green helium-neon laser was used to excite the fluorescent dye with a 15- μ m-diameter focused spot, and subcellular V_m were recorded optically during field stimulation directed along the long axis of the cell. The membrane response was measured at the cell end with the use of a 30-ms S1-S2 coupling interval and a 10-ms S2 pulse with strength of up to \sim 500-mV half-cell length potential (field strength \times one-half the cell length). The general trends show that 1) the response of V_m at the cell end occurs in two stages, the first being very rapid (<1 ms) and the second much slower in time scale, 2) the rapid response consists of hyperpolarization when the cell end faces the anode and depolarization when the cell end faces the cathode, 3) the rapid response varies nonlinearly with field strengths and polarity, being relatively larger for the hyperpolarizing responses, and 4) the slower, time-dependent response has a time course that varies in slope with field strength. Furthermore, the linearity of the dye response was confirmed over a voltage range of -280 to $+140$ mV by simultaneous measurements of optically and electrically recorded V_m . These experimental findings could not be reproduced by the updated, Luo-Rudy dynamic model but could be explained with the addition of two currents that activate outside the physiological range of voltages: a hypothetical outward current that activates strongly at positive potentials and a second current that represents electroporation of the cell membrane.

voltage-sensitive dye; Luo-Rudy model; electroporation; cardiac electrophysiology; computer model

ELECTRICAL STIMULATION of cardiac muscle is a common practice in clinical and academic medicine to pace, cardiovert, or defibrillate the heart. The mechanisms by which the electric field stimulus affects the transmembrane potential (V_m) of cardiac cells have been investigated theoretically, but experimental evidence is limited. A detailed study of how an external electric field affects a single cardiac myocyte is an important step toward understanding how electric fields affect the whole heart.

The costs of publication of this article were defrayed in part by the payment of page charges. The article must therefore be hereby marked "advertisement" in accordance with 18 U.S.C. Section 1734 solely to indicate this fact.

The cellular response during field stimulation has been explored in detail in passive spheroidal and cylindrical cell models (2, 9) and, more specifically, in cardiac cell models with active membranes (6, 12–14, 18, 19, 26). Single cells are predicted to respond to an external field in two stages. The first stage takes place immediately after the external field is turned on and consists of a differential charging of the cell membrane such that the end of the cell facing the cathode depolarizes and the end facing the anode hyperpolarizes. The membrane charging is a function of specific membrane capacitance and series resistance through the intracellular and extracellular spaces (2, 26) and occurs on a time scale of microseconds. As the cell membrane attains its reciprocal polarization, ionic channels are gated differentially by the V_m , resulting in a highly nonuniform flow of ionic currents into and out of the cell. The integral of the currents can result in a net flow of charge that causes the intracellular potential to change (13, 26). This second stage occurs over a much slower time scale, on the order of many milliseconds. When field stimuli are applied at rest, the net ionic current that is activated is inward and results in a net depolarization of the cell, leading to an action potential if excitation threshold is exceeded (26).

To monitor these events experimentally, optical indicators of V_m are necessary for at least two reasons. First, unlike electrodes, they are free from electrical stimulus artifacts that may easily arise when currents are applied to the tissue (21). Second, unlike microelectrodes, they provide the spatial resolution that is necessary to monitor the V_m at different parts of the cell (10, 30). However, optical studies of this type on single cardiac cells have been few and are not highly detailed. Experiments by Knisley and co-workers (10, 11) on single rabbit ventricular myocytes showed that field pulses applied during the action potential plateau induced depolarization and hyperpolarization at the cell ends with a magnitude that was roughly correlated to the product of field strength and cell length. Nevertheless, their data were unclear as to the degree of symmetry in the responses, the time-dependent changes that occurred during the stimulus pulse, and the quantitative relation between field intensity and response amplitude as field strength is varied. A preliminary report by Windisch and co-workers (29) on guinea pig ventricular myocytes showed a symmetrical variation in V_m along the length of the cell during field stimulation at rest at a single field strength, although the strength was not reported. The goal of this study, then, was to use voltage-sensitive dyes to obtain detailed, quantitative measurements of the subcellular changes in the V_m of adult ventricular myocytes induced by electric field stimulation. A second goal of this study

was to compare the measurements thus obtained with computational models of cells undergoing field stimulation as a test of the predictive accuracy of the models.

METHODS

Single-cell isolation and staining procedure. Guinea pigs (~250 g, Hartley strain) were given an intraperitoneal injection of 0.3 ml of pentobarbital sodium solution (50 mg/ml, Abbott Laboratories, Chicago, IL). The heart was removed by a thorotomy, quickly mounted on a perfusion setup, and retrograde perfused through the aorta with Ca^{2+} -free Tyrode solution for 7 min and then with enzyme solution for 3 min. The composition of Ca^{2+} -free Tyrode solution (in mM) was 135 NaCl, 5.4 KCl, 1 MgCl_2 , 0.33 NaH_2PO_4 , 5 HEPES, and 5 glucose (adjusted to pH 7.4 with NaOH); enzyme solution was Ca^{2+} -free Tyrode solution with 0.2 mM CaCl_2 , 0.1 mg/ml protease (type XIV, 5.5 U/mg; catalog no. P-5147, Sigma Chemical, St. Louis, MO), and 1 mg/ml BSA (catalog no. A-2153, Sigma Chemical). After digestion, the cardiac tissue was cut into small pieces and stirred in 5 ml of enzyme solution for 3 min and filtered with a 70- μm -pore filter. The filtered supernatant with isolated cells was then diluted by a factor of 5 with Tyrode solution containing 1.8 mM CaCl_2 . For optical recordings, cells were stained with the voltage-sensitive dye di-8-ANEPPS (10 μM ; Molecular Probes, Eugene, OR; stored in DMSO stock solution at 10 mM) for 5 min at room temperature (0.1% DMSO final).

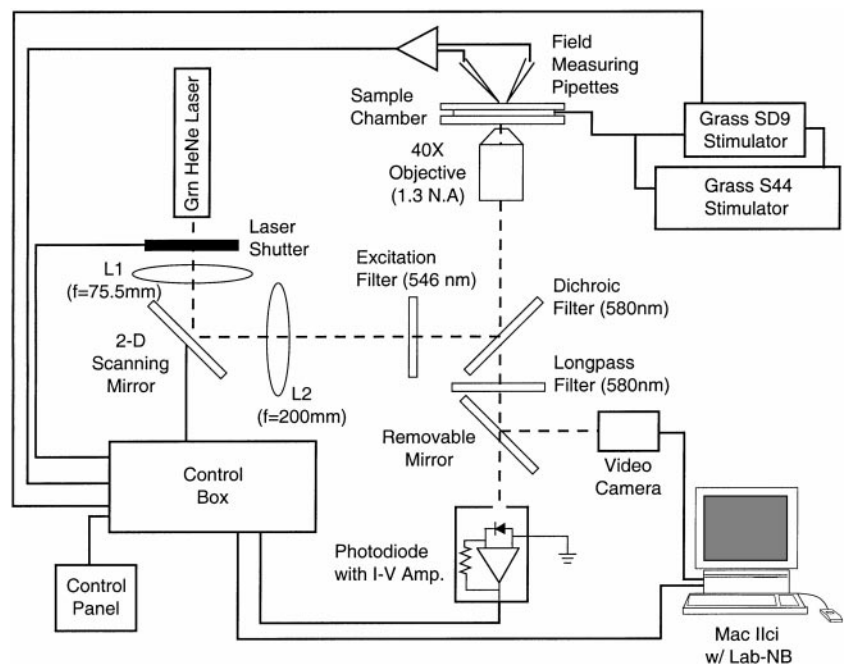
Experimental setup. A schematic diagram of the experimental system is shown in Fig. 1. The optical path is shown with dashed lines, and the electrical system with solid lines. Light from the excitation source, a 543-nm 1.5-mW green He-Ne laser (model 05-LGR-171, Melles Griot, San Marcos, CA), was gated by a bistable mechanical shutter (model 846HP, Newport, Irvine, CA) to minimize photobleaching and phototoxic effects. The laser was turned on for ≥ 20 min before experiments to allow stabilization of the beam output. The beam was steered by a two-dimensional galvomotorized mirror (model 6800/CB6580, Cambridge Technologies, Watertown, MA), passed through a 546 ± 7.5 -nm interference filter, reflected off a dichroic beam splitter (model DM580, Nikon,

Tokyo, Japan), and focused by an objective (Fluor $\times 40$, 1.3 NA, Nikon) onto a cardiac myocyte stained by fluorescent voltage-sensitive dye. The laser beam was expanded by a factor of f_2/f_1 with use of two biconvex lenses, L1 ($f_1 = 75.6$ mm, 1-in. diameter) and L2 ($f_2 = 200$ mm, 2-in. diameter), separated by a distance of 275.6 mm, to fill $\sim 80\%$ of the back aperture of the objective. This resulted in a 15- μm spot size in the specimen plane. L2 was placed 1,533 mm from the back aperture of the objective with use of a pair of adjustable mirrors, and the galvomotorized mirror was positioned at the conjugate plane for the back aperture (230 mm from L2) to keep the center rays orthogonal to the specimen plane and to prevent light from being blocked by the objective when the laser spot was moved.

Fluorescent light collected from the myocyte was then filtered through a long-pass filter (580 nm, model BA580, Nikon) to further attenuate residual excitation light. Finally, at the end of the optical path the fluorescent light was measured with a photodiode (model S2386-5K, Hamamatsu, Bridgewater, NJ) coupled to a high-gain current-to-voltage amplifier (model OPA111, Burr-Brown, Tucson, AZ) and a 1-G Ω feedback resistor (Eltec Instruments, Daytona Beach, FL). To limit overshoot and ringing of the amplifier, a small capacitor was formed with a Teflon-insulated wire-wrap wire and added to the feedback path by soldering one end to the output lead of the amplifier and wrapping the other end around the input of the amplifier with insulation intact. The step response of the amplifier circuit was tested with a fast light-emitting diode and had a rise time (10–90%) of 0.97 ms. Baseline fluorescent signals (F) were sampled with a sample-and-hold circuit and subtracted from the raw fluorescence signal to yield the V_m -dependent change in fluorescence (ΔF). The ΔF was then amplified 10 times and filtered with a 1-kHz low-pass single-pole filter before digitization by the computer (Lab NB board, National Instruments, Austin, TX) driven by LabVIEW software (National Instruments) running on a Macintosh IIci (Apple Computer, Cupertino, CA).

Control circuits for the experimental system were custom designed to provide timing signals for the laser shutter, data acquisition system, sample-and-hold circuit, and stimulus

Fig. 1. Schematic of optical recording system. Shutter-gated beam from a green He-Ne (Grn HeNe) laser was steered by a 2-dimensional (2-D) scanning mirror and reflected from a dichroic beam splitter. Reflected beam was focused by an objective onto a subcellular region (15- μm diameter) of a cardiac myocyte stained with fluorescent voltage-sensitive dye. Fluorescent signal was collected through the same objective and passed through a dichroic and a long-pass filter. Filtered signal was converted proportionally to an electrical signal through a photodiode and custom-built preamplifier circuit. A video camera was used to record size and orientation of cell. Two stimulators were used to excite the cell. Glass pipettes were pulled with ~ 10 - μm tips to measure electric field near cell. I - V , current-voltage; L1 and L2, lenses.



pulses. The laser shutter was opened for up to 400 ms and timed to begin before the start of the data acquisition. The sampling interval for the sample-and-hold circuit was 40 ms, and stimulus pulses were 10 ms in duration.

Field stimulation procedure. Approximately 30 μl of solution containing isolated, di-8-ANEPPS-stained guinea pig ventricular myocytes were placed into a field stimulation chamber (Fig. 2A) containing 1 ml of 1.8 mM Ca^{2+} -containing Tyrode solution at room temperature. Two stimulators (models SD9 and S44, Grass Instruments, Quincy, MA) were used to excite the myocytes with locally uniform electric field in the bath solution through a pair of parallel platinum wires (0.010-in. diameter) 4.5 mm long and 6.5 mm apart. Small S1 field stimulus pulses (10-ms-duration rectangular pulse with magnitude at 10% above diastolic threshold of ~ 3.6 V/cm) were turned on from one of the stimulators to pace the cells at 0.2 Hz. An isolated cardiac cell was located under the microscope using a $\times 10$ objective and then aligned at $\times 40$ with the laser excitation spot so that the edge of one of the longitudinal ends of the cell lay within the laser spot (Fig. 2B). Only cells that lay parallel to the electric field and contracted during stimulation were selected. After an experiment on a particular cell, the cells in the chamber were discarded and replaced by a fresh droplet of cells. Glass field recording pipettes (~ 10 - μm -diameter tip) were filled with 1.8

mM Ca^{2+} -containing Tyrode solution and inserted into the bath. The field recording pipettes were oriented ~ 300 μm apart parallel to the long axis of the cell and positioned laterally ~ 200 μm away from the cell. The cells and field recording pipettes were viewed with a video camera (model JE7362, Javelin Electronics, Los Angeles, CA) under bright-field or Hoffman modulation contrast optics, from which the cell length and spacing between the pipettes could be determined.

During each experimental recording, the repetitive pacing stimuli were turned off. An S1-S2 field stimulation procedure was used to quantify the electric field-induced hyperpolarization and depolarization at the ends of the cell. An S1 pulse (10 ms rectangular) from one of the stimulators was used to elicit an action potential. An S2 pulse (10 ms rectangular) from the other stimulator was timed to occur during the action potential plateau 30 ms after the onset of the S1 pulse and was set at a different amplitude every time. S1 and S2 polarities were always set to be in the same direction. In this study we define the stimulus to the cell in terms of the half-cell length potential (HCLP), where HCLP is the product of electric field strength and one-half the cell length. A negative HCLP indicates a field orientation from the end (being observed) toward the center of the cell (resulting in hyperpolarization of the end), and a positive HCLP indicates a field orientation in the opposite direction (resulting in depolarization of the end).

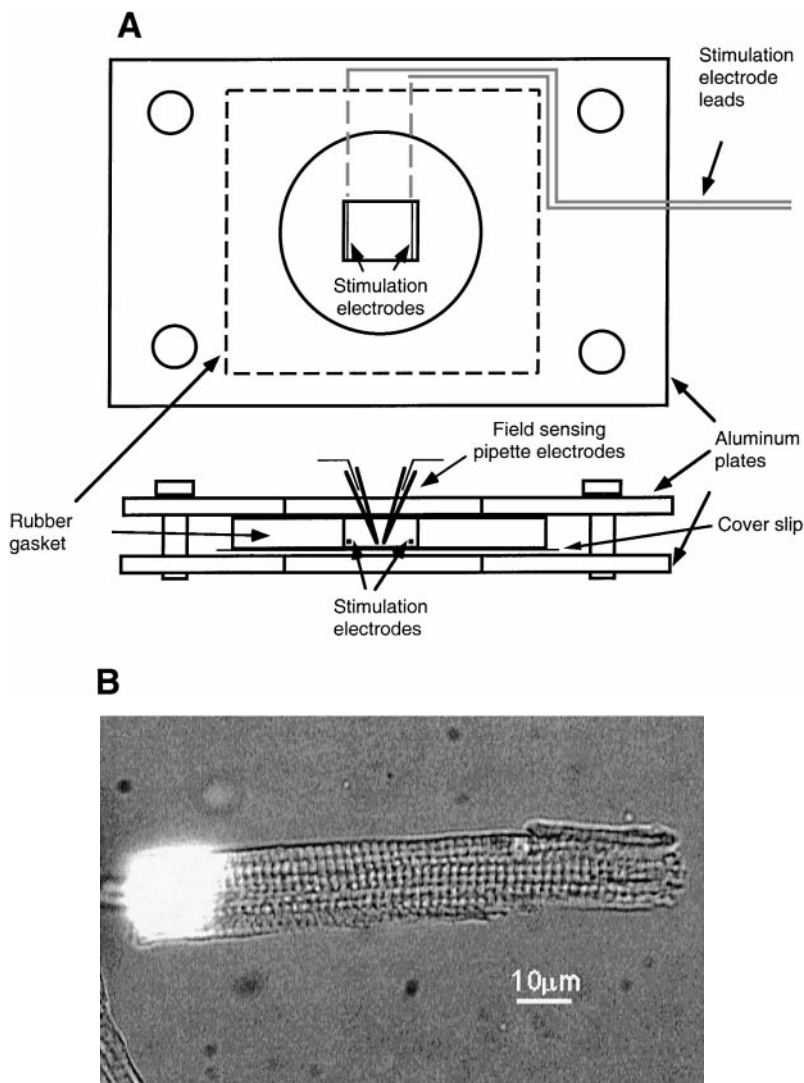


Fig. 2. Experimental chamber and single cell. *A*: schematic of experimental chamber. Chamber was formed by a rubber gasket overlying a square coverslip, sandwiched together between 2 aluminum plates. Stimulus electrodes consisted of 2 parallel 0.010-in.-diameter, 4.5-mm-long platinum wires separated by a distance of 6.5 mm. Two glass pipettes were filled with bath solution, and their potential difference was measured with Ag-AgCl wires to determine the applied field strength. *B*: bright spot on single guinea pig ventricular myocyte is laser-induced di-8-ANEPPS fluorescence of cell membrane. Transmembrane potential at end of cell could be recorded during field stimulation by acquiring the fluorescent signal at this spot with photodiode. Photomicrograph was obtained using Hoffman modulation contrast optics.

The reasons for using HCLP are twofold: 1) the HCLP is a normalized quantity that accounts for variations in cell length (10), and 2) for cells lying in a conductive bath and oriented along the electric field, the HCLP is the theoretical potential that develops at the end of the cell provided that the cell exerts only a minor perturbation of the applied field (2, 9, 26). For long, narrow cells this is a reasonable approximation. With this method of expressing the field strength, data from cells of different sizes can be combined and compared. The strength of S2 was varied from -400 - to $+510$ -mV HCLP. The change in fluorescence (ΔF) from the $\times 10$ amplifier stage, total fluorescence (F) from the photodiode preamplifier circuit, voltage from the field recording glass pipette electrodes, and stimulus current (measured across a $10\text{-}\Omega$ resistor in series with the platinum wire electrodes) were recorded. S1-S2 trials were repeated on the same cell until the cell was damaged by phototoxic effects or by field-induced injury caused by very large HCLP. Injured cells were identified by the onset of spontaneous contractions and in the extreme case by hypercontraction at the cell end.

In the experiments of this study, the optical response to fields with varying intensities and polarities was generally recorded at one end of the cell. The alternative procedure would have been to record responses sequentially at both ends of the cell for fields with various intensities but a single polarity. This latter type of experiment was not routinely performed for the bulk of the study because the accurate repositioning of the spot was difficult once the experiment was started, and accessibility to the microscope controls was difficult because the entire experimental setup was enclosed in a light-tight box. However, the results of one such experiment are included in this report.

Whole cell clamp. Additional experiments were conducted to calibrate optically recorded dye responses against electrically recorded V_m by using whole cell voltage clamp with a patch-clamp amplifier (model PC-One, Dagan, Minneapolis, MN). The bathing solution was changed to one containing a mixture of channel blockers along with elevated K^+ (in mM): 120 potassium glutamate, 25 KCl, 1 $MgCl_2$, 1 $BaCl_2$, 10 tetraethylammonium, 5 4-aminopyridine, 0.005 tetrodotoxin, 0.010 nifedipine, 0.5 $CdCl_2$, 0.1 EGTA, 10 HEPES, and 10 glucose (adjusted to pH 7.4 with HCl). A bathing solution of this composition was used to inactivate as many channels as possible and to reduce the ionic current across the cell membrane, which at high levels can produce significant errors between the applied command signal and the true V_m owing to voltage drops across the resistance of the pipette electrode (30). The solution in the pipette electrode consisted of (in mM) 110 potassium glutamate, 5 NaCl, 5 $MgCl_2$, 5 MgATP, 10 EGTA, and 5 HEPES (adjusted to pH 7.2 with KOH), resulting in a pipette resistance on the order of $5\text{--}10\text{ M}\Omega$.

After the successful attachment of the pipette electrode to the cell, the laser shutter was manually turned on. The laser spot was moved onto the cell close to the tip of the glass pipette and quickly turned off. The voltage-clamp waveform consisted of a series of rectangular pulse triplets with test potentials varying over a range of -400 to $+400$ mV. Each triplet consisted of an initial 10-ms clamp to -95 mV (near resting potential), a 10-ms clamp to $+35$ mV (near plateau potential), and a third 10-ms clamp to the test potential. This triplet protocol was designed in part to mimic how the membrane potential changes during S2 field stimulation. Moreover, the clamp potential always cycled through the same resting and plateau potentials for each triplet to allow for a two-point calibration with each test pulse. Thus it was possible to correct for any time-dependent change in the

fluorescence signal owing to photobleaching effects or to motion artifact over the duration of the entire voltage-clamp series. Simultaneous optical and electrical recordings were obtained, and ΔF , F, clamp voltage, and clamp current were recorded.

Computer simulations. Detailed model studies of field stimulation of cardiac cells having active membranes have been conducted for stimuli applied during diastole (14, 26) or during the relative refractory period (6, 12, 14). However, none of these studies have focused on the spatial and temporal patterns of the V_m within the cell as field strength is varied. Therefore, computer simulations of an isolated cardiac myocyte in a uniform electric field with various intensities were conducted for the purposes of comparison with the experimental data. The reciprocal polarization model for field stimulation has been described in detail previously (22, 26). Briefly, the cell was assumed to be a $120\text{-}\mu\text{m}$ -long, $24\text{-}\mu\text{m}$ -wide prolate spheroid, and the imposed field was assumed to be directed along the cell's major axis. During the stimulus the extracellular surface potentials were determined by the applied field, and the intracellular space was assumed to remain isopotential. The cell membrane was discretized into 11 patches, and the voltage-dependent ionic currents that developed in each of the patches led to further changes in V_m . Each membrane patch was assigned the kinetics of the updated Luo-Rudy dynamic (LRd) model of the guinea pig ventricular cell (16, 32). The model was implemented in Advanced Continuous Simulation Language (Mitchell and Gauthier, Concord, MA) on a Silicon Graphics (Mountain View, CA) POWER Challenge XL minisupercomputer. The nonlinear differential equations that govern the cellular response were solved iteratively using a second-order Runge-Kutta-Fehlberg algorithm with a variable step size of $\leq 10\ \mu\text{s}$.

RESULTS

S1-S2 field stimulation. The V_m estimated by optical means is denoted in this study as V_m^F . The optically measured action potential amplitude (APA^F) was determined by using the upstroke phase of the action potential as a calibration signal equal to 128 mV, the mean value of the action potential amplitude for isolated adult guinea pig ventricular myocytes (28, 30). Changes in V_m and V_m^F during the field stimulus are designated ΔV_m and ΔV_m^F , respectively. An example of V_m^F during S1-S2 field stimulation is shown in Fig. 3A. One end of the cell was monitored for stimulus fields of various intensities and polarities. Guinea pig ventricular cell lengths were in the range of 128 ± 23 (SD) μm ($n = 14$). The S2 response consists of a rapid, initial stage that occurs in < 1 ms. In this example, it is clear that for fields of opposite polarity the amplitude of the field-induced hyperpolarization is larger than the amplitude of depolarization at a comparable field strength by a factor of 1.54 at an HCLP of 70 mV and 3.29 at 180 mV (after correction for the slight differences in intensities for the 2 field polarities). The same experiment also shows marked differences in maximum upstroke velocity [$(dV_m^F/dt)_{\text{max}}$] of the action potentials elicited by the S1 pulses with a strength of 26.8-mV HCLP (Fig. 3A, *left*). The $(dV_m^F/dt)_{\text{max}}$ was 23.5% faster for the average of the two hyperpolarizing S1 pulses than the average of the two depolarizing pulses. This observation is consistent with the notion that the rapid upstroke of the action potential reflects the change in the average

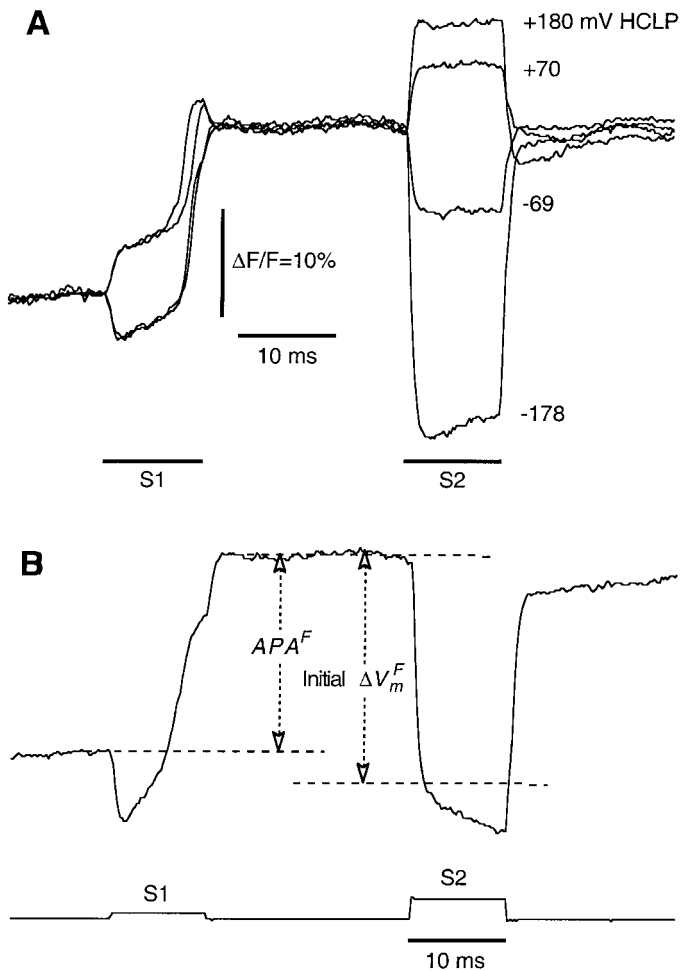


Fig. 3. Field-induced polarization changes. *A*: optical transmembrane potentials were measured at the same end of a single guinea pig ventricular cell before and after reversal of S1 and S2 field directions. Resulting hyperpolarized and depolarized responses are shown. S1 intensity was 4.7 V/cm; cell length was 114 μm . S2 field intensities were ~ 12 and 32 V/cm, and stimulus strength is expressed as half-cell length potential (HCLP, field intensity \times one-half cell length). S1 and S2 polarities were always in the same direction. Fields with same intensity but opposite polarities cause an asymmetrical response during action potential plateau. *F*, fluorescence. *B*: parameters used for data analysis. Action potential amplitude and response to stimulus field were quantified from the fluorescence signal. APA^F is action potential amplitude and is always positive. Initial ΔV_m^F is amplitude of S2 response at point of inflection relative to amplitude just before S2 stimulus and is negative for hyperpolarizing responses and positive for depolarizing responses.

potential of the cell but can be modulated from one end of the cell to the other by the reciprocal polarization of the membrane induced by the field stimulus (30).

The field-induced ΔV_m^F was analyzed as shown in Fig. 3*B*. The initial amplitude of ΔV_m^F was measured as the peak magnitude of V_m^F in the depolarizing direction or as the point of inflection in the hyperpolarizing direction, with both relative to the value just before the onset of the S2 pulse. This calculation resulted in an estimate of the field-induced ΔV_m (in mV) at the end of the cell. Figure 4*A* shows the composite results from eight different cells in which the initial ΔV_m^F (at the onset of the S2 pulse) is plotted against HCLP. Also

plotted in Fig. 4*A* is a dashed line with unity slope, which represents the ΔV_m^F expected for a cell with a membrane impedance much larger than that of the surrounding bath and an intracellular volume that is isopotential (26). Just as in Fig. 3*A*, the composite results show that the initial ΔV_m^F varies nonlinearly with field intensity and that the V_m is overhyperpolarized with one polarity and underdepolarized with the other at large values of HCLP compared with the straight-line response. The data are relatively linear over the range of -100 - to $+50$ -mV HCLP and can be fit using a least-squares error with the line $\Delta V_m^F = -2.280 + 0.780 \times \text{HCLP}$ ($R = 0.974$). In some cells, ΔV_m^F

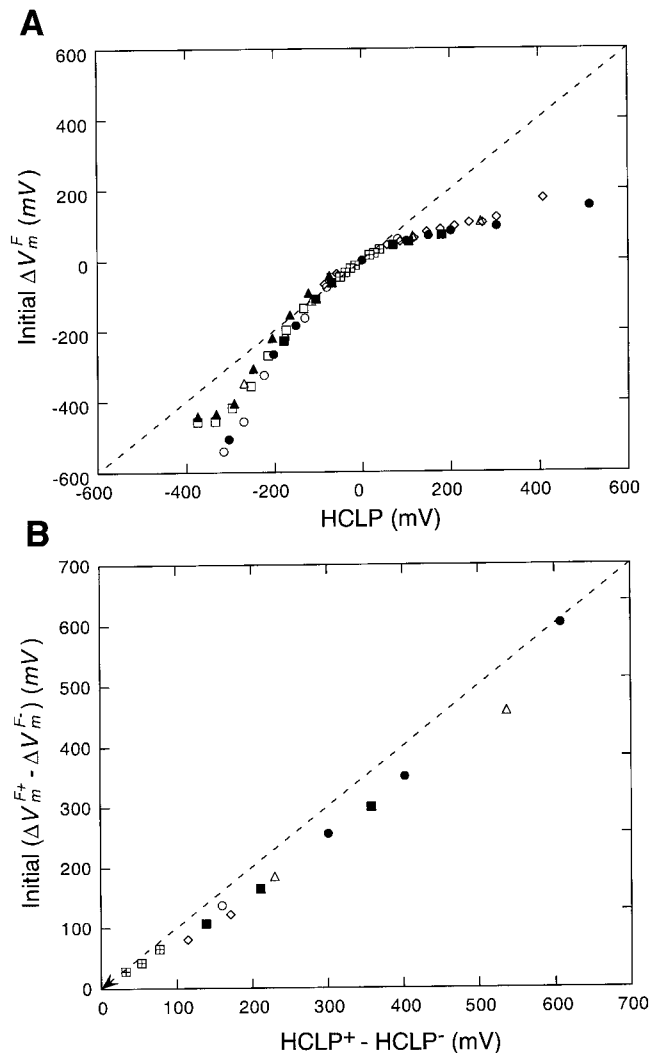


Fig. 4. Field-induced membrane response. *A*: initial ΔV_m^F at cell end plotted against HCLP during S2 field stimulation. Initial value of membrane response ΔV_m^F (estimated in mV) was calculated assuming an action potential amplitude of 128 mV. Plot represents data pooled from 8 myocytes, as indicated by different symbols (data from Figs. 3*A* and 5 are included). Dashed line, line of identity that is expected if cell membrane were to behave as a passive insulator with impedance much higher than that of bathing solution. *B*: for those cells that were stimulated by fields of both polarities and with approximately the same intensity, the difference between ΔV_m^{F+} and ΔV_m^{F-} for the 2 polarities HCLP⁺ and HCLP⁻, respectively, is plotted against HCLP⁺ - HCLP⁻. Data from different cells are indicated by symbol set used in *A*.

was recorded for both polarities of field stimuli. In those cases the total ΔV_m^F (equal to the difference between the 2 ΔV_m^F values) was plotted against the difference between the two HCLPs (sum of their magnitudes; Fig. 4B). Also plotted is a dashed line with unity slope that represents the total ΔV_m^F expected under ideal passive conditions (see DISCUSSION), as in the case for Fig. 4A. The points are close to but slightly below the line of identity and, with the exception of the point around +600 mV, can be fit by a straight line: $(\Delta V_m^F)_{\text{tot}} = 0.837 * (\text{HCLP}^+ - \text{HCLP}^-)$ ($R = 0.997$).

The S2 response also consists of a second, slower stage that occurs over the duration of the S2 pulse. The magnitude and slope of the slower response are shown in detail in Fig. 5 and vary with the field intensity. Responses in the depolarizing direction are shown in Fig. 5A from a single cell for HCLPs ranging from 100 to 510 mV. After the initial depolarization at the beginning of the pulse, ΔV_m^F fell in the hyperpolarizing

direction at an HCLP field intensity of 100 mV, remained relatively constant at 201 mV, and rose in the depolarizing direction at 304 mV. At 514 mV, ΔV_m^F fell again and was followed by a postshock depression of the action potential plateau. Responses in the hyperpolarizing direction are shown in Fig. 5B for a different cell for HCLP field intensities ranging from -81 to -316 mV and were directionally similar in slope to the depolarizing responses of Fig. 5A. ΔV_m^F fell in the hyperpolarizing direction at an HCLP of -130 mV, remained relatively constant at -223 mV, and rose in the depolarizing direction at -316 mV. The -316-mV shock was followed by a postshock depression of the action potential plateau. Larger hyperpolarizing responses were difficult to measure owing to injury effects. During very intense field stimulation (>400-mV hyperpolarizing HCLP), we observed that cells always hypercontracted at the hyperpolarized end. If the field direction was then reversed, hypercontracture was observed at the previously depolarized but now hyperpolarized end.

Calibration of di-8-ANEPPS. To check the linearity of the response of the dye di-8-ANEPPS, we attempted to record optical and electrical measurements simultaneously in the same cell. This was very difficult to perform and was successful in only one attempt. The command potential that was used is shown in Fig. 6A and consisted of a series of 33 shock triplets, with each triplet consisting of three 10-ms pulses in succession. The first pulse was at -90 mV, the second at +35 mV, and the third at a variable amplitude V_t . The V_m^F values from the first two pulses were used to calibrate the V_m^F measured with the third (test) pulse (Fig. 6B) and eliminated the need to assume a value for the action potential amplitude. When V_m^F was plotted against V_t , the data were fit well by a line having a slope of nearly unity (0.961, $R = 0.997$) over the range of -280 to +140 mV (Fig. 6C).

Responses at the center of the cell. To gain additional insight into the nature of the asymmetrical responses of Fig. 4 and to verify further that the responses were not an artifact of an asymmetry of the dye response for large polarization changes, ΔV_m^F was recorded at the center position of two cells to determine whether this site also mirrored the hyperpolarizing behavior seen at the cell ends. Figure 7 shows ΔV_m^F in one such experiment compared with responses in the same cell at each of the two ends. The ΔV_m^F values at the two ends are qualitatively similar to those at one end of a cell when the field polarity is reversed (Fig. 3A) and show an asymmetry in the hyperpolarizing direction for the larger responses. ΔV_m^F at the center hyperpolarizes rapidly with time (as indicated by the arrow) and then continues to decline slowly in the hyperpolarization direction. The significance of this finding is discussed below. As in Fig. 3A, these data also show that the upstroke velocity of the action potential varies with the polarization of the membrane and is 27.8 and 30.0% faster for the center and hyperpolarized end of the cell, respectively, than for the depolarized end.

Cell model simulations. Computer simulations were performed of an LRd model cell that was field stimu-

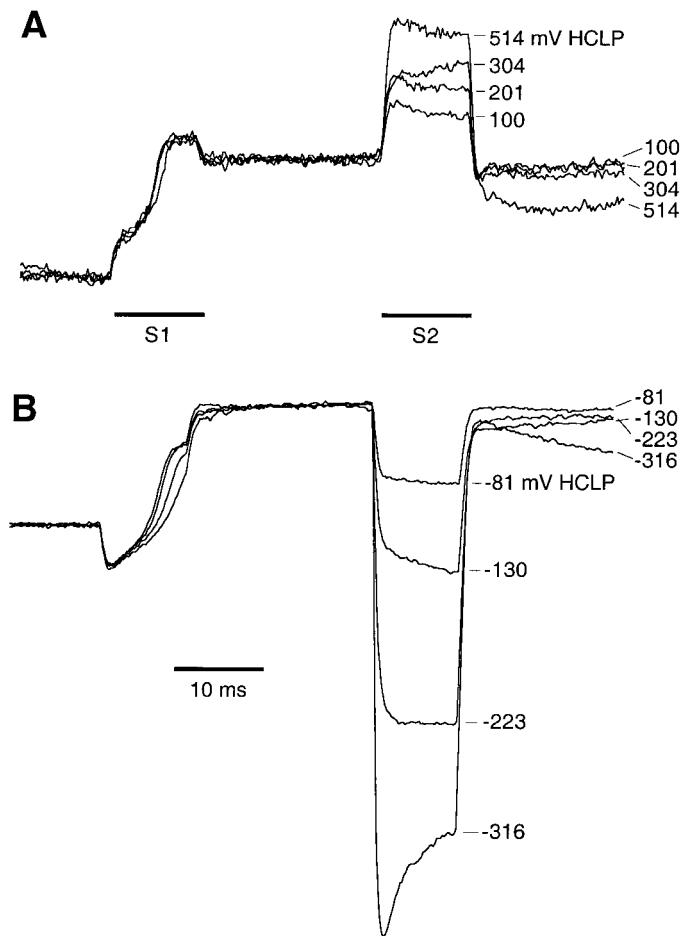


Fig. 5. Field-induced polarization of cell membrane. A 10-ms S1 field pulse was used to elicit an action potential in a guinea pig ventricular cell. When S2 field stimuli were applied during the action potential plateau, the anodal end of the cell hyperpolarized and the cathodal end depolarized. Polarities of S1 and S2 field stimuli were always in the same direction. Initial ΔV_m^F and time course of ΔV_m^F varied with S2 field strength. A: multiple recordings from cathodal end of a 156- μm -long single cell. B: multiple recordings from anodal end of a 173- μm -long different cell. S2 field strengths, expressed in units of HCLP, are indicated at right of their respective responses.

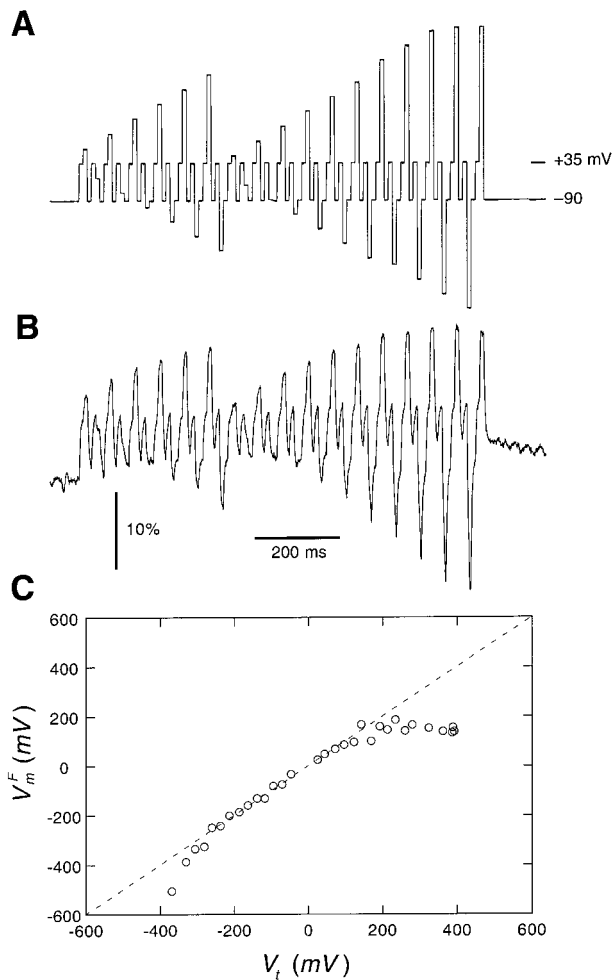


Fig. 6. Simultaneous optical and electrical recordings during voltage clamp. A whole cell voltage clamp of a guinea pig ventricular cell was used to calibrate dye di-8-ANEPPS in a guinea pig ventricular myocyte. *A*: a chopped rectangular pulse train was used (*top trace*), in which a series of 33 triplets of 10-ms pulses was applied. Each triplet consisted of a clamp to -90 mV, followed by a clamp to $+35$ mV, followed by a clamp to a test potential in the range -440 to $+390$ mV. *B*: simultaneously recorded V_m^F . *C*: V_m^F plotted against test potential (V_t). A nearly linear response of dye with slope of 0.961 was obtained for V_m^F in the range -280 to $+140$ mV ($R = 0.997$).

lated with a 5-ms S1 pulse followed by a 10-ms S2 pulse at a coupling interval of 30 ms with three representative field strengths (Fig. 8A). The model not only fails to reproduce the asymmetry of responses in the hyperpolarizing direction that were observed experimentally (Figs. 5 and 7) but exhibits an asymmetry in the opposite (depolarizing) direction at all field strengths when measured at the end of the S2 pulse. Moreover, at high field strengths the model fails to reproduce the depression of the action potential plateau, as was observed experimentally (Fig. 5), and instead shows a decaying depolarized response. These discrepancies can be resolved by postulating two currents that activate outside the physiological voltage range for which the LRd model was developed: a hypothetical time-independent outward current I_a and a current I_{ep} associated with electroporation of the cell membrane. We refer to the LRd model, modified by the addition of

these two currents, as the LRdm model. I_a was assumed to have the form (in $\mu\text{A}/\mu\text{F}$)

$$I_a = \begin{cases} e^{0.09(V_m - 100)}, & V_m \leq 160 \text{ mV} \quad (1a) \\ e^{0.09 \cdot 60} [0.09(V_m - 160) + 1], & V_m > 160 \text{ mV} \quad (1b) \end{cases}$$

and is plotted in Fig. 8C. The effect of I_a is to introduce the hyperpolarizing asymmetry seen in the traces for ± 200 -mV HCLP in Fig. 8B owing to activation of this outwardly rectifying current at the depolarized end of the cell.

To account for the depolarizing (ascending slope) ΔV_m^F seen in the traces for -316 - and $+304$ -mV HCLP in Fig. 5, as well as the postshock depression of the plateau potential observed at -316 - and $+514$ -mV HCLP also in Fig. 5, a second current is proposed. It is known that when V_m exceeds 300–400 mV across membrane patches, electroporation of the patch can occur (25). Recently, an electroporation current I_{ep} was formulated by DeBruin and Krassowska (4) to describe the saturation of V_m that develops at the ends of guinea pig muscle strips that are stimulated by electric fields

$$I_{ep} = N g_p V_m \quad (2a)$$

where the conductance of a single electropore (g_p) is a nonlinear, instantaneous function of V_m and the number of pores per unit area (N) has a growth rate given by

$$\frac{dN}{dt} = \alpha e^{\beta V_m^2} \left(1 - \frac{N}{N_0} e^{-q\beta V_m^2} \right) \quad (2b)$$

where N_0 is the equilibrium density of pores at $V_m = 0$ and α , β , and q are model constants. When added with

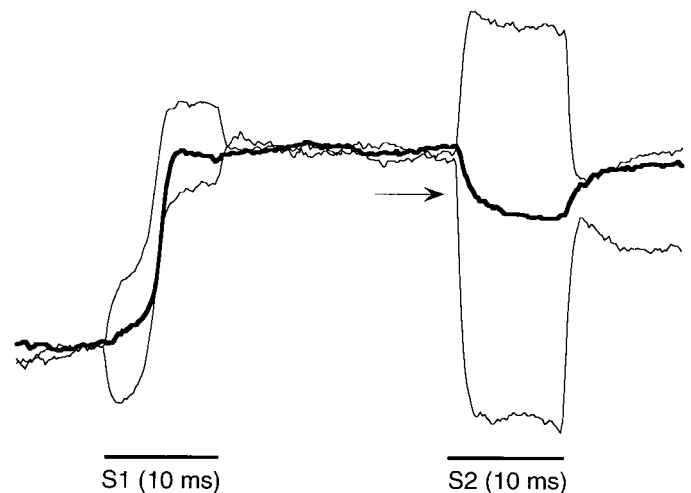
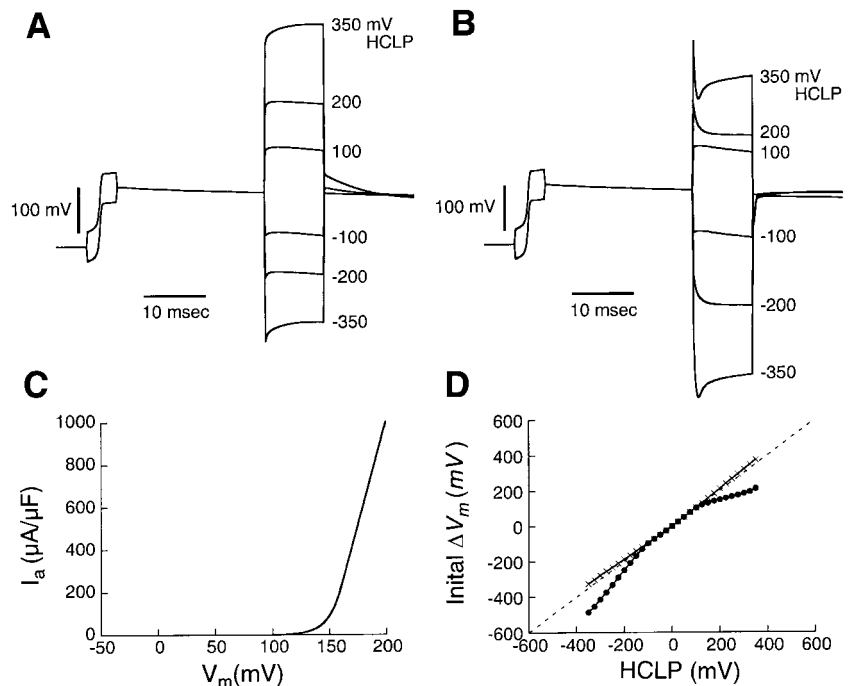


Fig. 7. Field-induced response at different parts of cell. V_m^F was measured at the center (bold trace) and ends (light traces) of a single guinea pig ventricular cell. A 10-ms S1 field pulse was used to excite cell, and then a second 10-ms S2 field pulse was used to elicit field response. S2 field strength in this experiment was not measured directly but is estimated to have been ~ 175 mV HCLP. S1 and S2 polarities were always set to be in the same direction. Individual traces exhibit small oscillations that may have resulted from a residual settling of the mechanical shutter of the excitation light source.

Fig. 8. Computer simulation of transmembrane potential response of cell to field stimulation. *A*: responses of both ends of a Luo-Rudy (LRd) model cell. A 5-ms rectangular S1 pulse was applied to model, and then a 10-ms S2 pulse was applied in same direction with an S1-S2 interval of 30 ms. Field intensities were 100-, 200-, and 350-mV HCLP. *B*: similar responses of an LRd model cell modified by addition of time-independent outward current (I_a) and electroperoration current (I_{ep}) (LRdm model cell), as given by Eqs. 1 and 2. These responses are hyperpolarized compared with corresponding responses in *A*. *C*: I - V relation of hypothetical ionic channel with current I_a . *D*: plot of initial field-induced response of end of cell as a function of field strength (in HCLP) analogous to Fig. 4A. Dashed line, passive response (line of identity); \times , responses of unaltered LRd model cell; \bullet , responses of LRdm model cell.



its published parameters to our LRd model simulations, I_{ep} becomes activated primarily at the hyperpolarized end of the cell during the S2 pulse, which produces the depolarizing ΔV_m^F seen in the traces for ± 350 -mV HCLP in Fig. 8*B*. The residual activation of I_{ep} also results in a small postshock depression of the plateau potential, consistent with the experimental observations.

The net effect of I_a and I_{ep} on the field responses at the end of the cell is shown in Fig. 8*D* for field strengths ranging from -350 - to $+350$ -mV HCLP. The dashed line is the line of identity, which is the result expected from purely passive models. Plotted is ΔV_m measured 1 ms after the onset of the S2 pulse. The curve obtained with the unmodified LRd model is nearly linear but with a slight upward concavity. The curve obtained with the LRdm model exhibits a downward concavity that reproduces the hyperpolarizing asymmetry that was observed experimentally (Fig. 4*A*).

DISCUSSION

This study used voltage-sensitive dyes to document the electrophysiological responses of single guinea pig ventricular myocytes to electric field stimulation during the plateau of the action potential. The main findings are as follows: 1) the response of the V_m at the cell end to the field occurs in two stages, the first being very rapid (<1 ms) and the second much slower in time scale, 2) the rapid response consists of hyperpolarization when the cell end faces the anode and depolarization when the cell end faces the cathode, 3) the rapid response varies linearly with HCLP field strengths from -100 to $+50$ mV and nonlinearly with higher strengths, being larger in magnitude than the HCLP at the hyperpolarized end and smaller than the HCLP at the depolarized end, and 4) the slower response has a

time course with a slope that varies with the field strength. 5) We also found that model simulations of an idealized cell with updated, Luo-Rudy dynamic properties fail to reveal the hyperpolarizing asymmetry that was observed experimentally but can be reconciled with the data by the addition of two membrane currents that activate outside the physiological voltage range.

Initial ΔV_m induced by an applied electric field. During excitation with rectangular field pulses, ΔV_m^F undergoes two characteristic stages of response. The first occurs during the 1st ms of the onset of the pulse (Fig. 3*B*), and the second occurs more slowly, over the full duration of the field pulse.

Concerning the first stage, at HCLP amplitudes between -100 and $+50$ mV we observed a linear relation between ΔV_m^F and field strength (Fig. 4*A*) and symmetrical changes with field polarity, as expected from theoretical models. For symmetrically shaped cells stimulated along their long axis by uniform fields, the cell end should respond linearly with field intensity, symmetrically in amplitude with field polarity, and symmetrically in amplitude with respect to the other end (2, 26). Symmetrically shaped cells stimulated by nonuniform fields (14) or arbitrarily shaped cells stimulated by uniform fields (13) are also expected to have responses at one end that are linear with field intensity and symmetrical with a reversal of field polarity, although the two ends of the cell should respond asymmetrically with respect to one other.

However, contrary to expectations, the relation between ΔV_m^F and HCLP has a slope of slightly <1 (0.78). The value of the slope is influenced by several competing factors. Because the measurement spot was not truly at the end of the cell but situated a distance up to a spot radius ($7.5 \mu\text{m}$) from the end, this would have led

to a consistent underestimate of ΔV_m^F . The value of 128 mV assumed for the action potential amplitude is a multiplicative factor for the slope and may have been in error. Finally, the effect of the cell to perturb the applied field is an additional factor that can change the slope, although this would have been in the opposite (increasing) direction and was assumed to be negligible in our analysis.

Higher levels of field intensity (less than -100 -mV HCLP or greater than $+50$ -mV HCLP), which at 50 -mV HCLP corresponds to ~ 8 V/cm for cells with mean length of 128 μm , resulted in a ΔV_m^F at the cell end that was larger in the hyperpolarizing direction when the field polarity was reversed (Fig. 3A). Moreover, the ΔV_m^F values at both ends of the cell and at the center of the cell shifted in the hyperpolarizing direction from the line of identity (Figs. 4 and 7).

Knisley and co-workers (10, 11) also reported asymmetrical ΔV_m^F at the opposite ends of the cell with field stimulation during the action potential plateau but found the changes to be nonsignificant. Nevertheless, the field intensities that they used (20 and 40 V/cm or HCLPs of 130 and 260 mV with the assumption that their cells are 130 μm long) should have placed their experiments well within the nonlinear region that we measured (Fig. 4). However, several differences exist between the study of Knisley et al. (10) and our study. First, their responses were averaged over a 25-ms window centered within a 50-ms S2 pulse and would have included some of what we have termed the slow second-stage response of the membrane. On this basis, we would have expected their recordings to have been even more asymmetrical than ours, but this was not the result reported. Another difference is that they measured changes in potential at the opposite ends of cells with a single polarity of field, whereas we generally measured the changes in potential at the same end of the cell with opposite polarities of field. As noted earlier, measurements at just one end may fail to reveal asymmetries that might otherwise be seen at the two ends, particularly for asymmetrical cell shapes or nonlinear fields. Thus the measurement procedure of Knisley et al. should have favored the observation of asymmetrical responses, contrary to the reported findings. A more likely explanation for the differences in the results is that the recordings of Knisley et al. were much noisier than ours and may have prevented a finding of statistical significance. Furthermore, their experiments were conducted on rabbit ventricular cells rather than guinea pig cells and, hence, may have involved different amounts or types of ionic currents that might contribute to the asymmetry (see below). Finally, their S1-S2 coupling interval was slightly longer (50 vs. 30 ms) and may have affected the degree of asymmetry, which has been shown to diminish with longer S1-S2 coupling intervals (7).

Optical mapping studies were conducted by Windisch and co-workers (30, 31) on single guinea pig cardiac cells and showed that ΔV_m^F varies spatially across the cell during field stimulation. In one preliminary experiment with an unspecified field strength, they reported a

spatially linear relation between polarization amplitude and position along the myocyte in the direction of the applied field (29). Such a relation is not incompatible with an asymmetrical ΔV_m^F at the end of the cell with a reversal in field polarity, provided that the linear relation is not symmetrical about the center of the cell. Additional experiments involving multisite optical mapping of cellular responses on a subcellular length scale are required to test this hypothesis.

As we reported earlier (27) and also showed in Fig. 8A, simulations based on passive models or on the active LRd model are unable to explain these consistent findings of a hyperpolarizing asymmetry. Given that existing models have been derived primarily from data in the physiological range, it may not be surprising for discrepancies to appear between experiment and model, particularly at the higher field intensities. A possible explanation for the discrepancy is that symmetrical responses are in fact occurring but are not faithfully recorded owing to the limited rise time (~ 1 ms) of our photodetector system. Indeed, the speed of the first-stage response is expected to be very fast, with a time constant equal to the product of specific membrane capacitance, a weighted sum of intracellular and extracellular resistivities, and the radius of the cell (2, 26). For typical values in cardiac cell membranes, this time constant is expected to be on the order of microseconds.

If indeed there is a symmetrical response that is being masked, then over the entire cell there must be a net outward current that rapidly activates and hyperpolarizes the intracellular potential. Thus the hyperpolarized end of the cell would become even more hyperpolarized, the depolarized end less depolarized, and the center hyperpolarized, as was observed experimentally (Fig. 7). This scenario was tested using a hypothetical current I_a that activates outside the normal physiological voltage range with the instantaneous, outwardly rectifying current-voltage relation shown in Fig. 8C. The addition of this current to the LRd model enables much of the experimentally observed behavior to be reproduced (Fig. 8B). Note that the very rapid transients predicted by the model at the onset of the S2 pulse would not be observable in the data because of the limited frequency response of the recording system.

If this explanation is correct, then according to our model simulations the augmentation of the hyperpolarization at one end of the cell and reduction of the depolarization at the other should be equal for a given field intensity. Expressed in another way, the difference between the ΔV_m^F values should equal the difference between the HCLPs, i.e., the extracellular potential difference from one end of the cell to the other, or the product of the field strength and the whole cell length. Although we did not map the responses simultaneously at the two ends of the cell, if we assume that the cell ends behave symmetrically with respect to one another, we can combine our data at one end of the cell for HCLPs with comparable magnitudes but opposite polarity. Our results fall close to the expected relation (Fig. 4B), although they are better fit with a line having a slope of slightly < 1 (0.84). The reasons for the lower

slope may be identical to those discussed earlier regarding the lower-than-expected slope of the linear region of the relation of Fig. 4A.

Thus a rapidly changing ionic conductance within the 1st ms of ΔV_m^F may account for the nonlinear and asymmetrical behavior of the membrane that is not otherwise accounted for by present-day theoretical models of cardiac cells undergoing field stimulation. This mechanism may also contribute to the asymmetrical ΔV_m^F values recorded optically (7, 33) and ΔV_m values recorded with microelectrodes (34) at the tissue level after reversal of the field stimulus polarity. Although we have demonstrated that a current such as I_a is consistent with the findings of asymmetry, further investigation is necessary to confirm the existence and nature of this current. Possible candidates for I_a may include Cl^- or K^+ currents, which have negative reversal potentials and can have outwardly rectifying current-voltage relations.

An alternative explanation for the asymmetry may be that the voltage-sensitive dye itself responds nonlinearly with V_m . Experiments were performed to test the linearity of the dye response by using the voltage-clamp method in conjunction with simultaneous optical recordings. As shown in Fig. 6, we found an excellent correlation between fluorescence intensity of di-8-ANEPPS and V_m over a range of -280 to $+140$ mV. Deviation of the data from a linear relationship outside this range of potentials might be attributed to the fact that, at the high amplitude potentials, not all ionic currents were blocked. Indeed, the voltage limits of the linear relation are approximately where we have hypothesized I_a and I_{ep} to activate. These currents may not have been eliminated by our mixture of channel blockers and could have led to a failure of V_m to be clamped to the command potential by virtue of the voltage drop across the pipette resistance (30) or of intracellular potential gradients along the cell length. In other studies, experiments on single frog ventricular cells also showed a nearly linear relation of V_m^F to V_m during the action potential or during ramp clamps in voltage over a range of -150 to $+150$ mV (3). With a similar dye (di-4-ANEPPS), experiments performed on guinea pig ventricular myocytes showed a linear relation between V_m^F and V_m over a range of -120 to $+40$ mV (30). A linear relation between di-4-ANEPPS fluorescence and V_m has also been demonstrated in other cell types (5, 8, 15, 17), over a range as large as -200 to $+200$ mV in HeLa cells (17). Regardless of the exact limits of linearity, the dye does appear to respond linearly with V_m , at least in the physiological range of V_m . Although we were not able to verify the linearity of response over the entire range of ΔV_m^F at the cell end (almost -600 to $+150$ mV; Fig. 4), the observation of a hyperpolarizing response at the center of the cell, which does remain within the physiological voltage range (Fig. 7), further supports the notion that the asymmetrical responses seen at the cell end with reversals in field polarity are true physiological changes and not an artifact of nonlinearities in dye response.

Time course of ΔV_m during field stimulus. As the field stimulus strength is increased, the time course of the slower, second-stage response of ΔV_m^F to the field pulse changes its slope in a consistent manner, regardless of the field direction or which end of the cell is being observed (Fig. 4). On theoretical grounds, a nonzero slope reflects a net imbalance of ionic currents from the different parts of the cell during field stimulation (13, 26). If the imbalance results in a net outward current, the isopotential interior of the cell will move in the negative direction. Because the profile of extracellular potential along the surface of the cell is essentially unchanged during the field stimulus, the average V_m of the cell will become more negative. This is seen with HCLPs on the order of ± 100 mV (Fig. 5). Indeed, our model simulations (Fig. 8) indicate that the net outward current arises because the sum total of ionic current exiting at the depolarized end of the cell exceeds the total current entering the hyperpolarized end (results not shown).

When the HCLP is raised to approximately ± 200 mV, the ΔV_m^F responses are essentially flat in time after the initial rapid response, indicating that the net sum of ionic currents over the entire cell membrane is zero. For even greater HCLPs on the order of ± 300 mV or more (Fig. 5), ΔV_m^F diminishes in hyperpolarization and becomes more positive during the latter part of the S2 pulse. The upward turn in ΔV_m^F measured at the higher field strengths could not be reproduced by the LRd model in combination with I_a and presumably results from an increase of an inward current and/or a decrease of an outward current. Previous work from our laboratory showed that electroporation of the cell membrane can occur with V_m in the range of 300 – 400 mV (25). When an I_{ep} (Eq. 2, *a* and *b*) was added along with I_a to the LRd model, the upward turn in ΔV_m^F and the postshock depression of the plateau potential were reproduced at high field strengths (cf. Figs. 5 and 8), since I_{ep} acts to drive V_m toward the short-circuit potential of 0 mV. Visual observations of cells by Knisley et al. (11) and by us have demonstrated that spontaneous contractions and hypercontracture occur first at the hyperpolarized end as field strength is increased, consistent with the entry of extracellular Ca^{2+} there via electroporation. Although Knisley et al. invoked electroosmosis together with electroporation as a mechanism to explain the asymmetry of Ca^{2+} entry with shocks given during the action potential plateau, our findings of a hyperpolarizing asymmetry in ΔV_m^F at the two ends of the cell suggest that electroporation by itself is consistent with the data, since it would occur first at the hyperpolarized end of the cell. At even higher field strengths, electroporation would be expected to occur at the depolarized end as well and would explain the downward turn in ΔV_m^F now seen at that end (Fig. 5). Knisley et al. also reported that ΔV_m^F decays toward zero potential at both ends of the cell at high field strengths (50 V/cm).

Although an I_{ep} is consistent with the upward turn in ΔV_m^F seen at the highest field strengths (Fig. 5), it is nonetheless still speculative, and other possibilities

exist. One possibility is that there is a hyperpolarization-activated inward current I_f and voltage-dependent block of the inward rectifier current I_{K1} , as described recently by Ranjan et al. (20). To test this idea, we ran additional simulations in which these currents were implemented in their published form together with I_a in the LRd model. However, the resulting effect of I_f on ΔV_m^F was relatively insignificant (results not shown) and unable to account for our experimental findings, despite the large magnitude of hyperpolarization achieved at the cell end. Another possibility is that, at the cell end undergoing hyperpolarization, large inward currents in the form of "tail currents," such as these from activated Ca^{2+} channels, could contribute to membrane depolarization as well as the contractile asymmetry commented on earlier. Clearly, further investigation is required to identify the precise ionic currents underlying the temporal aspects of ΔV_m during the field stimulus.

Responses to field stimuli applied at rest. Although this study focused on the responses of the membrane to field stimuli of various amplitudes that are applied during the early plateau of the action potential, our data also reveal the responses to field stimuli applied during rest. In Fig. 3A the membrane response to the S1 field pulse can be seen at the left side of the traces. The end of the cell exhibits a rapid change in potential at the onset and cessation of the S1 stimulus pulse, similar to the response during the plateau to the S2 pulse. However, the slower second-stage responses exhibit a pronounced depolarization that reaches threshold followed by a rapid depolarization and upstroke. From a previous modeling study (26) and as shown in Fig. 8, such a depolarizing response is expected to occur as a result of net inward currents arising from the nonlinear conductive properties of the inward rectifier K^+ channel combined with activation of the Na^+ channel. The same study also predicted that the fast Na^+ current would be larger at the hyperpolarized than at the depolarized end of the cell. The present experimental results support this prediction and show the maximum upstroke velocity to be 23.5–30.0% faster for membrane patches that are hyperpolarized than for those that are depolarized by the field stimulus (Figs. 3A and 7). An elegant experimental mapping study by Windisch and co-workers (30) showed that the upstroke velocity of the action potential varies linearly with the amplitude of the membrane polarization produced by the field pulse, being fastest at the hyperpolarized end and slowest at the depolarized end.

Limitations of the study. The main drawback of this study is that V_m^F values were not measured simultaneously across the cell owing to the nature of our recording system (single spot measurements). Hence, several expectations derived from theoretical models remain unproven. For example, the potential changes during the slower stage of polarization are expected to parallel one another in field-stimulated cells (13, 14, 26). This behavior is characteristic not only of single cells but also of tissue in which virtual sources of opposite polarity may exist in close proximity to one

another, with a separation on the order of a space constant or less (1, 23, 24). Figure 7 suggests that this expected behavior does occur in the single cell, although the data were not obtained simultaneously for the same field stimulus, so that some changes in the state of the cell might have occurred between recordings. In experiments on guinea pig myocytes, Windisch et al. (30) recorded potentials from multiple sites simultaneously across the cell and showed parallel shifts in potential, although measurements were made only during diastole. Further research is necessary to determine whether such changes also occur during other phases of the action potential and for what range of field intensities this behavior exists.

We are grateful to Robert Susil for assisting with the development of the computer simulations and to Matthew Fishler and Vinod Sharma for comments regarding the manuscript.

This work was supported by National Heart, Lung, and Blood Institute Grant HL-48266.

Much of this work was performed as part of a master's dissertation (3) and was presented in abstract form (27).

Address for reprint requests and other correspondence: L. Tung, Dept. of Biomedical Engineering, The Johns Hopkins University, Rm. 703, Traylor Bldg., 720 Rutland Ave., Baltimore, MD 21205 (E-mail: ltung@bme.jhu.edu).

Received 20 July 1998; accepted in final form 9 March 1999.

REFERENCES

1. **Cartee, L. A., and R. Plonsey.** The effect of cellular discontinuities on the transient subthreshold response of a one-dimensional cardiac model. *IEEE Trans. Biomed. Eng.* 39: 260–70, 1992.
2. **Cartee, L. A., and R. Plonsey.** The transient subthreshold response of spherical and cylindrical cell models to extracellular stimulation. *IEEE Trans. Biomed. Eng.* 39: 76–85, 1992.
3. **Cheng, D.** *Optical Measurements of Transmembrane Potential Change During Electrical Field Stimulation of Isolated Cardiac Myocytes* (Master's thesis). Baltimore, MD: Johns Hopkins University, 1996.
4. **DeBruin, K. A., and W. Krassowska.** Electroporation and shock-induced transmembrane potential in a cardiac fiber during defibrillation strength shocks. *Ann. Biomed. Eng.* 26: 584–596, 1998.
5. **Ehrenberg, B., D. L. Farkas, E. N. Fluhler, Z. Lojewska, and L. M. Loew.** Membrane potential induced by external electric field pulses can be followed with a potentiometric dye. *Biophys. J.* 51: 833–837, 1987. [Corrigenda. *Biophys. J.* 52: July 1987, following p. 141.]
6. **Fishler, M. G., E. A. Sobie, N. V. Thakor, and L. Tung.** Mechanisms of cardiac cell excitation with premature monophasic and biphasic field stimuli—a model study. *Biophys. J.* 70: 1347–1362, 1996.
7. **Gillis, A. M., V. G. Fast, S. Rohr, and A. G. Kléber.** Spatial changes in transmembrane potential during extracellular electrical shocks in cultured monolayers of neonatal rat ventricular myocytes. *Circ. Res.* 79: 676–690, 1996.
8. **Gross, D., L. M. Loew, and W. W. Webb.** Optical imaging of cell membrane potential changes induced by applied electric fields. *Biophys. J.* 50: 339–348, 1986.
9. **Klee, M., and R. Plonsey.** Stimulation of spheroidal cells—the role of cell shape. *IEEE Trans. Biomed. Eng.* 23: 347–354, 1976.
10. **Knisley, S. B., T. F. Blitchington, B. C. Hill, A. O. Grant, W. M. Smith, T. C. Pilkington, and R. E. Ideker.** Optical measurements of transmembrane potential changes during electric field stimulation of ventricular cells. *Circ. Res.* 72: 255–270, 1993.
11. **Knisley, S. B., and A. O. Grant.** Asymmetrical electrically induced injury of rabbit ventricular myocytes. *J. Mol. Cell. Cardiol.* 27: 1111–1122, 1995.

12. **Krassowska, W., and M. S. Kumar.** The role of spatial interactions in creating the dispersion of transmembrane potential by premature electric shocks. *Ann. Biomed. Eng.* 25: 949–963, 1997.
13. **Krassowska, W., and J. C. Neu.** Response of a single cell to an external electric field. *Biophys. J.* 66: 1768–1776, 1994.
14. **Leon, L. J., and F. A. Roberge.** A model study of extracellular stimulation of cardiac cells. *IEEE Trans. Biomed. Eng.* 40: 1307–1319, 1993.
15. **Loew, L. M., L. B. Cohen, J. Dix, E. N. Fluhler, V. Montana, G. Salama, and J. Y. Wu.** A naphthyl analog of the aminostyryl pyridinium class of potentiometric membrane dyes shows consistent sensitivity in a variety of tissue, cell, and model membrane preparations. *J. Membr. Biol.* 130: 1–10, 1992.
16. **Luo, C.-H., and Y. Rudy.** A dynamic model of the cardiac ventricular action potential. I. Simulations of ionic currents and concentration changes. *Circ. Res.* 74: 1071–1096, 1994.
17. **Montana, V., D. L. Farkas, and L. M. Loew.** Dual-wavelength ratiometric fluorescence measurements of membrane potential. *Biochemistry* 28: 4536–4539, 1989.
18. **Platzer, D., E. Hofer, and H. Windisch.** Modeling geometrical aspects in cardiac stimulation and propagation experiments. *Proc. Annu. Int. Conf. IEEE Eng. Med. Biol. Soc.* 17: 710–711, 1995.
19. **Quan, W., and T. J. Cohen.** Field stimulation of single cardiac cell—the dependency of membrane excitation threshold on waveform shape and cellular refractoriness. *Proc. Annu. Int. Conf. IEEE Eng. Med. Biol. Soc.* 15: 869–870, 1993.
20. **Ranjan, R., N. Chiamvimonvat, N. V. Thakor, G. F. Tomaselli, and E. Marban.** Mechanism of anode break stimulation in the heart. *Biophys. J.* 74: 1850–1863, 1998.
21. **Salama, G.** Optical measurements of transmembrane potential in heart. In: *Spectroscopic Membrane Probes*, edited by L. Loew. Boca Raton, FL: CRC, 1988, p. 137–199.
22. **Sobie, E. A., and L. Tung.** Post-shock potential gradients and dispersion of repolarization in cells stimulated with monophasic and biphasic waveforms. *J. Cardiovasc. Electrophysiol.* 9: 743–756, 1998.
23. **Susil, R. C., E. A. Sobie, and L. Tung.** Virtual source separation modulates cardiac tissue response to field stimulation. *Proc. Annu. Int. Conf. IEEE Eng. Med. Biol. Soc.* 19: 182–184, 1997.
24. **Susil, R. C., E. A. Sobie, and L. Tung.** Separation between virtual sources modifies the response of cardiac tissue to field stimulation. *J. Cardiovasc. Electrophysiol.* 10: 715–727, 1999.
25. **Tovar, O., and L. Tung.** Electroporation and recovery of the cardiac cell membrane with rectangular voltage pulses. *Am. J. Physiol.* 263 (*Heart Circ. Physiol.* 32): H1128–H1136, 1992.
26. **Tung, L., and J. R. Borderies.** Analysis of electric field stimulation of single cardiac muscle cells. *Biophys. J.* 63: 371–386, 1992.
27. **Tung, L., D. K. Cheng, R. Susil, and E. A. Sobie.** Electrical field excitation of cardiac cells—matching theory to experiment (Abstract). *Ann. Biomed. Eng.* 24: S-57, 1996.
28. **Watanabe, T., P. M. Rautaharju, and T. F. McDonald.** Ventricular action potentials, ventricular extracellular potentials, and the ECG of guinea pig. *Circ. Res.* 57: 362–373, 1985.
29. **Windisch, H., H. Ahammer, P. Schaffer, W. Müller, and M. Hartbauer.** Optical micromapping reveals potential distributions on cardiomyocytes during field stimulation. *Proc. Annu. Int. Conf. IEEE Eng. Med. Biol. Soc.* 17: 714, 1995.
30. **Windisch, H., H. Ahammer, P. Schaffer, W. Müller, and D. Platzer.** Optical multisite monitoring of cell excitation phenomena in isolated cardiomyocytes. *Pflügers Arch.* 430: 508–518, 1995.
31. **Windisch, H., W. Müller, H. Ahammer, P. Schaffer, D. Dapara, and M. Hartbauer.** Optical potential mapping helps to reveal discrete-natural-phenomena in cardiac muscle. *Int. J. Bifurc. Chaos* 6: 1925–1933, 1996.
32. **Zeng, J., K. R. Laurita, D. S. Rosenbaum, and Y. Rudy.** Two components of the delayed rectifier K^+ current in ventricular myocytes of the guinea pig type. Theoretical formulation and their role in repolarization. *Circ. Res.* 77: 140–152, 1995.
33. **Zhou, X., R. E. Ideker, T. F. Blitchington, W. M. Smith, and S. B. Knisley.** Optical transmembrane potential measurements during defibrillation-strength shocks in perfused rabbit hearts. *Circ. Res.* 77: 593–602, 1995.
34. **Zhou, X., D. L. Rollins, W. M. Smith, and R. E. Ideker.** Responses of the transmembrane potential of myocardial cells during a shock. *J. Cardiovasc. Electrophysiol.* 6: 252–263, 1995.